

REFERENCES AND NOTES

- W. Dansgaard *et al.*, *Nature* **364**, 218 (1993); Greenland Ice-core Project Members, *Nature* **364**, 203 (1993); P. M. Grootes, M. Stuiver, J. W. C. White, S. Johnsen, J. Jouzel, *ibid.* **366**, 552 (1993); M. Stuiver, P. M. Grootes, T. F. Braziunas, *Quaternary Res.* **44**, 341 (1995).
- R. B. Alley *et al.*, *Nature* **362**, 527 (1993).
- E. J. Brook, T. Sowers, J. Orhardo, *Science* **273**, 1087 (1996); J. Chappellaz *et al.*, *Nature* **366**, 443 (1993); P. A. Mayewski *et al.*, *Science* **261**, 195 (1993).
- G. Bond *et al.*, *Nature* **365**, 143 (1993); S. J. Lehmann and L. D. Keigwin, *ibid.* **356**, 757 (1992); K. A. Hughen, J. T. Overpeck, L. C. Peterson, S. Trumbore, *ibid.* **380**, 51 (1996); R. J. Behl and J. P. Kennett, *ibid.* **379**, 243 (1996).
- L. D. Keigwin and G. A. Jones, *J. Geophys. Res.* **99**, 12397 (1994); W. B. Curry and D. W. Oppo, *Paleoceanography* **12**, 1 (1997).
- A. E. Bainbridge, *GEOSECS Atlantic Ocean Expedition, Vol. 2, Sections and Profiles* (Government Printing Office, Washington, DC, 1980).
- E. A. Boyle and L. D. Keigwin, *Science* **218**, 784 (1982); D. Oppo and R. G. Fairbanks, *Earth Planet. Sci. Lett.* **86**, 1 (1987); *Paleoceanography* **5**, 277 (1990).
- E. A. Boyle and L. D. Keigwin, *Nature* **330**, 35 (1987).
- J. C. Duplessy *et al.*, *Paleoceanography* **3**, 343 (1988).
- M. Sarnthein *et al.*, *ibid.* **9**, 209 (1994).
- D. W. Oppo and S. J. Lehman, *Science* **259**, 1148 (1993).
- J. E. Smith, M. J. Risk, H. P. Schwarcz, T. A. McConaughy, *Nature* **386**, 818 (1997).
- H. Cheng, J. F. Adkins, R. L. Edwards, E. A. Boyle, unpublished data.
- S. D. Cairns and G. D. Stanley Jr., *Proc. Fourth Int. Coral Reef Symp. Manila* **1**, 611 (1981).
- Age screening was done by measuring ^{230}Th , ^{232}Th , and ^{238}U by isotope dilution in cleaned samples on an inductively coupled plasma-mass spectrometer at the Massachusetts Institute of Technology.
- R. L. Edwards *et al.*, *Science* **260**, 962 (1993).
- Samples were cleaned of exterior organic carbon and coatings of manganese/iron oxides with successive leaches in a 50:50 mixture of 30% peroxide and 1 M NaOH. A final short leach in a 50:50 mixture of peroxide and 1% perchloric acid was used to remove all remaining organic stains. These precleaning steps removed 15 to 25% of the original coral weight. Immediately before final dissolution and graphitization, corals were soaked in 10% HCl to remove an additional 7 to 30% of aragonite. This procedure overcomes contamination problems from modern carbon that result from storage and handling and organic carbon from polyp and crust material. Samples were carefully chosen to avoid secondary calcification from endolithic activity.
- The $^{14}\text{C}/^{12}\text{C}$ ratio is expressed with the Δ notation, where $\Delta^{14}\text{C}$ is the per mil deviation from the $^{14}\text{C}/^{12}\text{C}$ ratio in 19th-century wood [M. Stuiver and H. A. Polach, *Radiocarbon* **19**, 355 (1977)].
- J. F. Adkins and E. A. Boyle, *Paleoceanography* **12**, 337 (1997).
- E. Bard *et al.*, *Earth Planet. Sci. Lett.* **126**, 275 (1994); W. E. N. Austin, E. Bard, J. B. Hunt, D. Kroon, J. D. Peacock, *Radiocarbon* **37**, 53 (1995); K. Gronvold *et al.*, *Earth Planet. Sci. Lett.* **135**, 149 (1995); H. H. Birks, S. Gulliksen, H. Hafliadason, J. Mangerud, G. Possnert, *Quaternary Res.* **45**, 119 (1996).
- E. Bard, M. Arnold, R. Fairbanks, B. Hamelin, *Radiocarbon* **35**, 191 (1993).
- W. S. Broecker, G. Bond, M. Klas, G. Bonani, W. Wolfli, *Paleoceanography* **5**, 469 (1990); G. E. Birchfield and W. S. Broecker, *ibid.* **5**, 835 (1990).
- M. Stuiver and H. G. Ostlund, *Radiocarbon* **22**, 1 (1980); W. S. Broecker, R. Gerard, M. Ewing, B. C. Heezen, *J. Geophys. Res.* **65**, 2903 (1960).
- We measured the spatial variation in Cd/Ca ratios from within a single modern *D. cristagalli* to check for vital effects. These biologically induced nonthermodynamic deviations from equilibrium for a particular tracer have been found to dominate the stable carbon and oxygen isotope signatures of deep-sea corals (12). A coral from 550 m in the South Pacific Ocean had an average Cd/Ca value of $0.172 \mu\text{mol/mol}$ with 1 SD of $0.016 \mu\text{mol/mol}$. There was no within-coral spatial pattern to this variation. Although *D. cristagalli* may contain vital effects for Cd/Ca, this 10% SD is smaller than the signal in JFA 24.8 and does not have the top-to-bottom coherence we find in the 15.4-ka sample. For these reasons we believe sample JFA 24.8 has faithfully captured a change in the [Cd] of the past water masses.
- The carbon isotopic ratio is defined as follows: $\delta^{13}\text{C} = [(^{13}\text{C}/^{12}\text{C})_{\text{sample}} / (^{13}\text{C}/^{12}\text{C})_{\text{standard}} - 1] \times 1000$, relative to the Pee Dee Belemnite standard [see H. Craig, *Geochim. Cosmochim. Acta* **3**, 53 (1953)].
- The coral Cd distribution coefficient is the ratio of Cd/Ca in the coral to Cd/Ca in the water. Similar to a core top calibration in foraminifera, we measured Cd/Ca ratios in a suite of modern *D. cristagalli* that span a range of 0.5 to $3.2 \mu\text{M} [\text{PO}_4]$. Six of these coral fall on a line with a slope of 1.6 coral per water Cd/Ca ratio. This value implies a $[\text{PO}_4]$ of $3.6 \mu\text{M}$ for the top of sample JFA 24.8. However, there are three other samples from this calibration that have significantly higher Cd/Ca ratios in the coral than was predicted by the water [Cd]. On the basis of this study, we believe the distribution coefficient for *D. cristagalli* is 1.6 or higher and that the $3.6 \mu\text{M} [\text{PO}_4]$ estimate for JFA 24.8 is a maximum value.
- W. S. Broecker, S. Blanton, M. Smethie Jr., G. Ostlund, *Global Biogeochem. Cycles* **5**, 87 (1991).
- H. Kitagawa and J. van der Plicht, *Science* **279**, 1187 (1998).
- S. J. Lehmann and L. D. Keigwin, *Nature* **356**, 757 (1992).
- S. Lehman, personal communication.
- L. D. Keigwin, G. A. Jones, S. J. Lehman, E. A. Boyle, *J. Geophys. Res.* **96**, 16811 (1991).
- AMS radiocarbon dates were measured by standard procedures at the Lawrence Livermore National Laboratory Center for Accelerator Mass Spectrometry (CAMS). Ventilation ages were calculated with the ^{14}C projection age method described in (79). In three of the corals there is a slight elevation in initial $\delta^{234}\text{U}$, indicating a small degree of exchange with a high $\delta^{234}\text{U}$ reservoir. From the observation that there is no significant correlation between ^{230}Th age and $\delta^{234}\text{U}$ in different fragments of the same coral (13), we infer that the effect of this exchange on ^{230}Th age is small.
- We thank S. Griffin, C. Masiello, and B. Grant for laboratory assistance. Discussions with D. Sigman, W. S. Broecker, and A. L. van Geen helped improve the manuscript. Supported by the National Science Foundation. J.F.A. was supported by a NASA Global Change fellowship and a grant from Tokyo Electric and Power Company.

18 November 1998; accepted 18 March 1998

Local Orbital Forcing of Antarctic Climate Change During the Last Interglacial

Seong-Joong Kim,* Thomas J. Crowley, Achim Stössel

During the last interglacial, Antarctic climate changed before that of the Northern Hemisphere. Large local changes in precession forcing could have produced this pattern if there were a rectified response in sea ice cover. Results from a coupled sea ice-ocean general circulation model supported this hypothesis when it was tested for three intervals around the last interglacial. Such a mechanism may play an important role in contributing to phase offsets between Northern and Southern Hemisphere climate change for other time intervals.

One of the perplexing problems in Pleistocene climatology involves the factors responsible for Antarctic climate change. Although orbital insolation variations play a major role in driving Pleistocene climate change (1), the precessional component of orbital forcing is almost out of phase between the Northern Hemisphere (NH) and Southern Hemisphere (SH), so any conditions favorable for glaciation and deglaciation in the NH should result in the opposite response in the SH. For more than 20 years it has been known that although SH cooling in the Pleistocene accompanied NH glaciation, SH climate led NH climate into and out of the last (and other) interglacials. That is, the SH warmed and cooled before the NH (1). Carbon dioxide also increased before NH glacial retreat (2). Yet standard

explanations for SH climate change rarely focus on local forcing changes around Antarctica. Most explanations involve more remote processes such as changes in atmospheric carbon dioxide concentration (3), variations in North Atlantic Deep Water (NADW) heat transport to the Antarctic (4), or lowering of sea level causing expansion of the Antarctic ice sheet. There is, however, a modest ($\sim 1^\circ\text{C}$) contribution from mean annual changes in the local radiation budget at the highest latitudes as a result of synchronous NH-SH obliquity changes at the 41,000-year period (5).

Here, we show that local forcing at the precessional period (19,000 and 23,000 years), which is out of phase between the NH and SH, may also be important in SH climate change. We based our study on the hypothesis that seasonal changes in the Antarctic summer may be proportionately more important than in the Antarctic winter because sea ice is much closer to the freezing point in summer. This relation may allow a

Department of Oceanography, Texas A&M University, College Station, TX 77843, USA.

*To whom correspondence should be addressed. E-mail: ksj@ocean.tamu.edu

rectified response to orbital insolation variations and may account for some of the phase offsets in climate change between the NH and SH. We tested our model with a coupled sea ice–ocean general circulation model (OGCM).

We used the Hamburg Ocean Primitive Equation (HOPE) model (6), which is based on the primitive equations with a prognostic free surface (7). The equations are discretized on the basis of the Arakawa-E grid (8), and the model has horizontal resolution of an effective 3.5° by 3.5°, with 11 vertical layers. The model includes a comprehensive dynamic-thermodynamic sea ice model (9). The ocean is forced by climatological monthly mean winds (10), except for the Southern Ocean sea ice, which is forced by daily winds from the European Center for Medium-Range Weather Forecast analyses. The treatment of surface temperature and salinity is dependent on the presence of sea ice. In ice-free grid cells, sea surface temper-

ature and salinity are relaxed to prescribed air temperature (11) and salinity (12).

To obtain the surface temperature response to the orbital insolation change during the Pleistocene, we used a linear version of an energy balance model (EBM) (13). This is a two-dimensional model that resolves the temperature response to seasonal insolation forcing as it is modified by geography. Although the EBM is a simplified model, numerous sensitivity experiments (14) indicate that its response to orbital insolation changes is approximately the same as that of atmospheric general circulation models. We chose three time periods (Fig. 1): 106 ka (thousand years ago) and 125 ka, at which local summer insolations are at minima (15), and 135 ka, at which summer insolation is at a maximum. These time intervals were chosen because at the beginning of the last interglacial (130 to 135 ka), CO₂ and temperature increased before NH ice sheet melting (2, 16), and temperature then decreased before NH ice growth (1). The mid- to high latitudes of the SH

cooled almost as much as at the glacial maximum at 106 ka. Earlier linear EBM calculations (Fig. 1) suggested that local orbital forcing could play an important role in phase shifts and seasonal cooling for these time periods, but some feedback would be required to translate the forcing into mean annual temperature changes, such as are estimated for the Vostok site (17).

The strongest EBM temperature responses occurred during the austral summer in the SH (Fig. 2). In January at about 80°S, simulated temperatures at 106 and 125 ka were about 3.9°C and 1.8°C lower than at present, respectively, whereas at 135 ka the temperature was ~1.4°C higher than at present. We then imposed these temperature differences on the climatological atmospheric forcing of the sea ice–ocean model to investigate the change in Antarctic ice area and the overturning circulation. The temperature changes were imposed only south of 45°S in order to isolate the mid- to high-latitude response of the SH to orbital insolation changes. After 600 years of integration, the model reached a quasi-steady

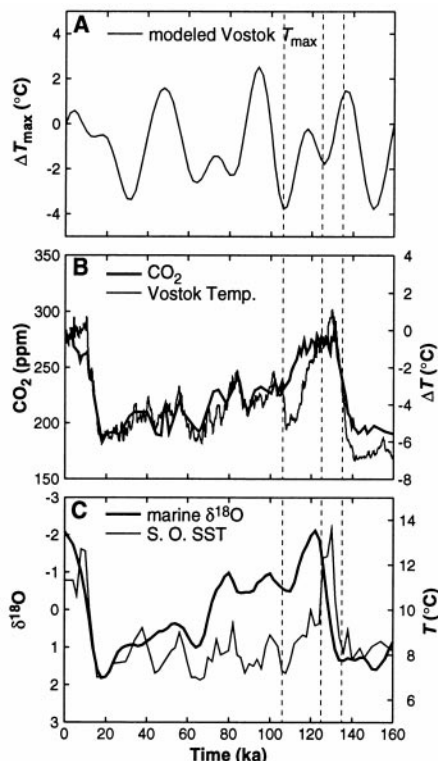


Fig. 1. Key climate records from the mid- and high latitudes of the Southern Hemisphere. (A) Simulated maximum summer temperatures T_{max} at 80°S [from (5)]. (B) Vostok (80°S) ice core CO₂ and temperature variations. (C) Estimated Southern Ocean sea surface temperatures (SST) at 45°S and deep sea $\delta^{18}O$ record (1). The ice core CO₂ and temperature are from (16) and (17); the time scale is ice core extended geological time (EGT) (17). Vertical dashed lines represent time intervals examined in this study. The slight offset between 45° and 80°S in the timing of the cooling event at 106 ka could be a chronology problem (2, 17), but it could also reflect real lags within the SH.

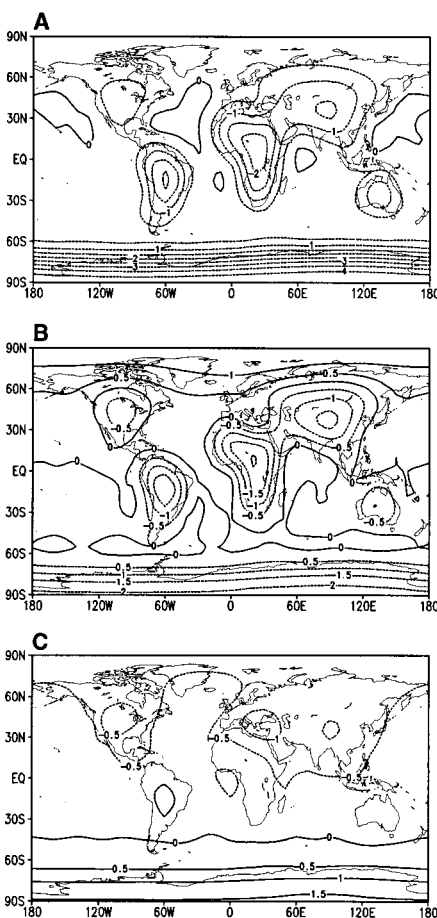


Fig. 2. Simulated January EBM temperature differences from control for 106 ka (A), 125 ka (B), and 135 ka (C). Dashed and solid lines represent cooling and warming with respect to the present, respectively.

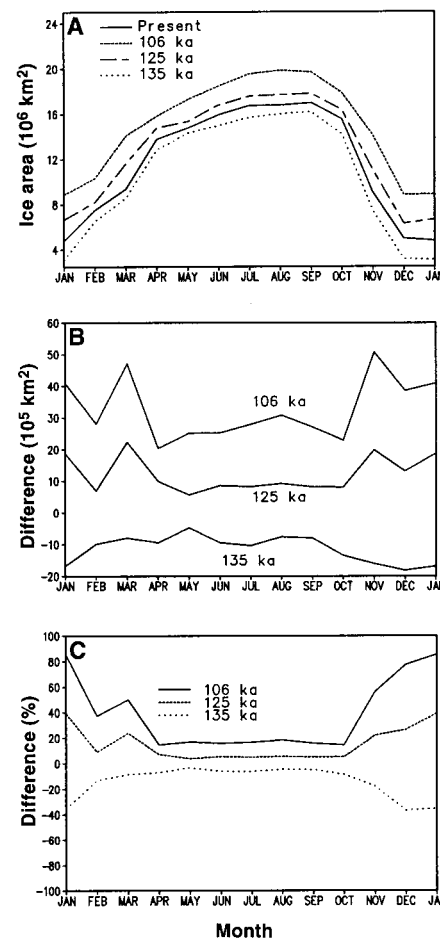


Fig. 3. Simulated seasonal variation of Antarctic sea ice area (A), ice area differences (B), and percent differences (C) from control for 106, 125, and 135 ka.

state; that is, the climate drift in temperature and salinity at all model levels was within the range of 0.01°C and 0.001 psu per century.

At present, the simulated Antarctic sea ice area varies from $\sim 4.5 \times 10^6$ km² in austral summer to $\sim 17 \times 10^6$ km² in austral winter (Fig. 3) (18). In the model, at 106 ka and 125 ka, the mean annual Antarctic ice area increased by 3.2×10^6 km² and 1×10^6 km², respectively, and at 135 ka it decreased by $\sim 1.1 \times 10^6$ km². The biggest difference was in austral summer (October to April), with a change of +80%, +40%, and -40% for 106 ka, 125 ka, and 135 ka, respectively. Inspection of model time series (19) indicates a systematic offset from the control run in sea ice area; that is, the differences do not appear to reflect model drift or centennial variability. For 125 ka, a mean annual cooling was also obtained for this region in a coupled model run (20), but

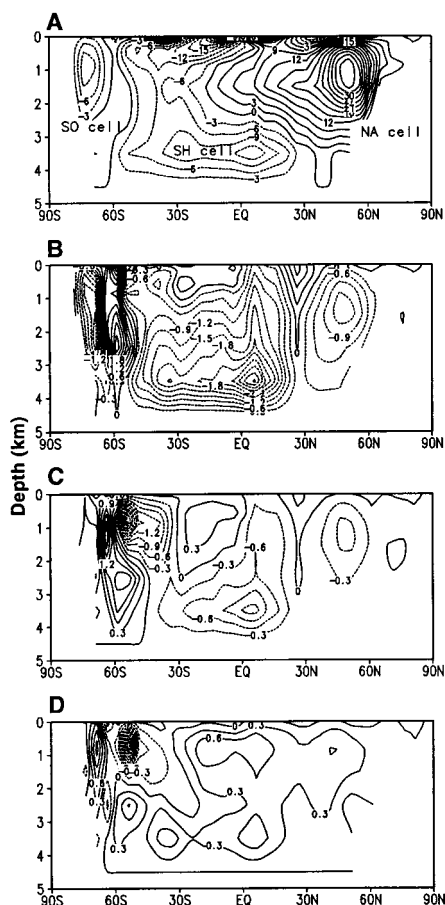


Fig. 4. (A) Present-day annual mean global meridional overturning circulation (SO, Southern Ocean; SH, Southern Hemisphere; NA, North Atlantic). (B to D) Differences in overturning circulation from 106 ka (B), 125 ka (C), and 135 ka (D). By convention, negative values in difference fields for SO intrusion indicate increased overturning circulation. Note that strong changes at about 60°S are attributable to slight meridional shifts of the SO cell.

that experiment used the full (global) orbital insolation change for this time interval.

Changes also occurred in the modeled thermohaline circulation (Fig. 4). The present-day Antarctic Bottom Water (AABW) intrusion across the equator is ~ 12 sverdrups (1 Sv = 1×10^6 m³/s), which is close to the flow obtained from a previous model study (21) and compares well with recent estimates (22, 23). The model overestimates the present-day formation of NADW (36 Sv) versus recent estimates from observed sections (27 Sv) (23), but NADW outflow at 30°S (19) is 17 Sv, which is realistic. For the 106 ka simulation, the AABW intrusion increased by 3.3 Sv, while the production of NADW decreased by 1.2 Sv. At 125 ka, the AABW intrusion increased by 1.5 Sv, and it decreased slightly by 0.6 Sv at 135 ka. The Pacific Basin records the largest change in deep Antarctic outflow, but this response may well be model dependent.

Geochemical data have been interpreted as indicating that variations of NADW contributed to Antarctic sea ice meltback during terminations (4). However, the role of NADW in terms of forcing SH climate has been challenged (24). Our results suggest that changing outflow of deep water from the Antarctic could change the relative abundance of northern component water at any particular site, leading to potential misinterpretations of past NADW variations.

Our results therefore support the hypothesis that the sea ice response to local Milankovitch forcing changes could affect both the timing and magnitude of climate change in the Southern Ocean. Modeled sea ice change could also conceivably affect CO₂ concentration (25), which would then further modify sea ice (3). This latter response might be particularly relevant to the early CO₂ rise at about 130 to 135 ka (Fig. 1), but additional feedbacks would be required to amplify the modest response we obtained for this time interval. For example, weaker winds in the Southern Ocean (26), caused by reduced sea ice, should decrease heat loss from the ocean (27) and increase sea surface temperatures. Ice-age surface (sea ice) conditions might also be more sensitive to insolation variations. These problems would have to be addressed with fully coupled models, which at present do not simulate high-latitude SH climates well (28) and are too computer-intensive to be used for a series of quasi-equilibrium sensitivity experiments.

REFERENCES AND NOTES

- J. D. Hays, J. A. Imbrie, N. J. Shackleton, *Science* **194**, 1121 (1976); J. Imbrie *et al.*, in *Milankovitch and Climate*, A. Berger *et al.*, Eds. (Reidel, Dordrecht, Netherlands, 1984), pp. 269–305; D. G. Martinson *et al.*, *Quat. Res.* **27**, 1 (1987); J. Imbrie, A. McIntyre,

- A. Mix, in *Climate and Geosciences: A Challenge for Science and Society in the 21st Century*, A. Berger, J.-C. Duplessy, S. H. Schneider, Eds. (Reidel, Hingham, MA, 1989), pp. 121–164; L. Labeyrie *et al.*, *Paleoceanography* **11**, 57 (1996).
- T. Sowers *et al.*, *Paleoceanography* **8**, 737 (1993); T. Sowers and M. Bender, *Science* **269**, 210 (1995).
- S. Manabe and A. J. Broccoli, *J. Atmos. Sci.* **42**, 2643 (1985).
- P. K. Weyl, *Meteorol. Monogr.* **8**, 37 (1968); J. Imbrie *et al.*, *Paleoceanography* **8**, 699 (1993).
- D. A. Short *et al.*, *Quat. Res.* **35**, 157 (1991).
- J. Wolff, E. Maier-Reimer, S. Legutke, *Report No. 13*, Deutsches Klimarechenzentrum (1997), p. 81.
- S. Drijfhout, C. Heinze, M. Latif, E. Maier-Reimer, *J. Phys. Oceanogr.* **26**, 559 (1996).
- A. Arakawa and V. R. Lamb, *Methods Comput. Phys.* **17**, 173 (1972).
- The sea ice dynamics adopt the viscous-plastic constitutive law of W. D. Hibler III [*J. Phys. Oceanogr.* **9**, 815 (1979)]; sea ice thermodynamics are adopted from W. B. Owens and P. Lemke [*J. Geophys. Res.* **95**, 9527 (1990)].
- S. Helleman and M. Rosenstein, *J. Phys. Oceanogr.* **13**, 1093 (1983).
- S. D. Woodruff, R. J. Slutz, R. L. Jenne, P. M. Streurer, *Bull. Am. Meteorol. Soc.* **68**, 1239 (1987).
- S. Levitus, *NOAA Prof. Pap.* **13** (1982).
- G. R. North, J. G. Mengel, D. A. Short, *J. Geophys. Res.* **88**, 6576 (1983).
- T. J. Crowley, D. A. Short, J. G. Mengel, G. R. North, *Science* **231**, 579 (1986); W. T. Hyde, T. J. Crowley, K.-Y. Kim, G. R. North, *J. Clim.* **2**, 864 (1989); T. J. Crowley, S. K. Baum, W. T. Hyde, *J. Geophys. Res.* **96**, 9217 (1991).
- A. L. Berger and M. F. Loutre, *Quat. Sci. Rev.* **10**, 297 (1991).
- J. M. Barnola, D. Raynaud, Y. S. Korotkevich, C. Lorius, *Nature* **329**, 408 (1987).
- J. Jouzel *et al.*, *ibid.*, p. 403; J. Jouzel *et al.*, *ibid.* **364**, 407 (1993).
- This is slightly overestimated over passive microwave observation [P. Gloersen *et al.*, *Arctic and Antarctic Sea Ice, 1978–1987* (Scientific and Technical Information Program, NASA, Washington, DC, 1992), p. 290], which shows that the Antarctic sea ice varies from $\sim 2 \times 10^6$ km² in austral summer to $\sim 15 \times 10^6$ km² in austral winter.
- S.-J. Kim, T. J. Crowley, A. Stössel, data not shown.
- M. Montoya, T. J. Crowley, H. von Storch, *Paleoceanography* **13**, 170 (1998).
- W. Cai and P. G. Bains, *J. Geophys. Res.* **101**, 14073 (1996); A. Stössel, S.-J. Kim, S. Drijfhout, *J. Phys. Oceanogr.*, in press.
- M. M. Hall, M. McCartney, J. A. Whitehead, *J. Phys. Oceanogr.* **27**, 1903 (1997).
- A. M. Macdonald and C. Wunsch, *Nature* **382**, 436 (1996).
- T. J. Crowley, *Paleoceanography* **7**, 489 (1992); T. Blunier *et al.*, *Geophys. Res. Lett.* **24**, 2683 (1997).
- J. R. Toggweiler and J. L. Sarmiento, in *The Carbon Cycle and Atmospheric CO₂: Natural Variations Archean to Present*, E. T. Sundquist and W. S. Broecker, Eds. (American Geophysical Union, Washington, DC, 1985), pp. 163–184; R. François *et al.*, *Nature* **389**, 929 (1997).
- M. DeAngelis, N. I. Barkov, V. N. Petrov, *Nature* **325**, 318 (1987).
- T. J. Crowley and C. L. Parkinson, *Clim. Dyn.* **3**, 93 (1988).
- J.-S. von Storch *et al.*, *J. Clim.* **10**, 1525 (1997); a climate drift also occurs in the National Oceanic and Atmospheric Administration/Geophysical Fluid Dynamics Laboratory-coupled model [S. Manabe and R. J. Stouffer, *ibid.* **9**, 376 (1996)], but the reason has not been identified.
- Supported by NSF grants OCE96-16977 and ATM 95-29109 and funding from Texas A&M University.

19 December 1997; accepted 16 March 1998